Laboratory emissivity measurements of the plagioclase solid solution series under varying environmental conditions

K. L. Donaldson Hanna,[1] I. R. Thomas,[2] N. E. Bowles,[2] B. T. Greenhagen,[3] C. M. Pieters,[1] J. F. Mustard,[1] C. R. M. Jackson,[1] and M. B. Wyatt[1]

Received 1 July 2012; revised 29 August 2012; accepted 27 September 2012; published 8 November 2012.

[1] New laboratory thermal infrared emissivity measurements of the plagioclase solid solution series over the 1700 $\sim$ 400 cm^{-1} (6–25 μm) spectral range are presented. Thermal infrared (TIR) spectral changes for fine-particulate samples (0–25 μm) are characterized for the first time under different laboratory environmental conditions: ambient (terrestrial-like), half-vacuum (Mars-like), vacuum, and vacuum with cooled chamber (lunar-like). Under all environmental conditions the Christiansen Feature (CF) is observed to vary in a systematic way with Na-rich end-member (albite) having a CF position at the highest wave number (shortest wavelength) and the Ca-rich end-member (anorthite) having a CF position with the lowest wave number (longest wavelength). As pressure decreases to $<10^{-3}$ mbar four observations are made: (1) the CF position shifts to higher wave numbers, (2) the spectral contrast of the CF increases relative to the RB, (3) the spectral contrast of the RB in the $\sim$1200–900 spectral range decreases while the spectral contrast of the RB in the $\sim$800–400 spectral range either increases or remains the same and (4) the TF disappears. A relationship between the wavelength position of the CF measured under simulated lunar conditions and plagioclase composition (An#) is developed. Although its exact form may evolve with additional data, this linear relationship should be applied to current and future TIR data sets of the Moon. Our new spectral measurements demonstrate how sensitive thermal infrared emissivity spectra of plagioclase feldspars are to the environmental conditions under which they are measured and provide important constraints for interpreting current and future thermal infrared data sets.

Citation: Donaldson Hanna, K. L., I. R. Thomas, N. E. Bowles, B. T. Greenhagen, C. M. Pieters, J. F. Mustard, C. R. M. Jackson, and M. B. Wyatt (2012), Laboratory emissivity measurements of the plagioclase solid solution series under varying environmental conditions, *J. Geophys. Res.*, *117*, E11004, doi:10.1029/2012JE004184.

1. Introduction

[2] Plagioclase feldspars are important mineral phases in intrusive igneous rocks such as anorthosites and extrusive igneous rocks such as basalts. Collected samples, meteorites, and remote sensing observations have identified plagioclase feldspars on terrestrial bodies throughout the inner solar system. Remote observations of the Martian surface by the Thermal Emission Spectrometer (TES) onboard Mars Global Surveyor (MGS) identified two surface lithologies that cover most of the surface (Surface Type1 and 2) that are both dominated by plagioclase feldspar [*Bandfield et al.*, 2000; *Hamilton et al.*, 2001; *Wyatt and McSween*, 2002]. Ground- and space-based telescopic thermal infrared observations of Vesta's surface indicate regions spectrally dominated by pyroxene and plagioclase mixtures [*Donaldson Hanna and Sprague*, 2009] or similar in composition to eucrite meteorites [*Mittlefehldt et al.*, 1998]. Samples returned from the Apollo missions provided evidence that the lunar highlands contain significant amounts of anorthosite (a rock containing >90% plagioclase) [e.g., *Wood et al.*, 1970; *Dowty et al.*, 1974]. Recent high spatial resolution data sets have identified regions in the lunar highlands that are composed purely of plagioclase [*Matsunaga et al.*, 2008; *Ohtake et al.*, 2009; *Pieters et al.*, 2009; *Donaldson Hanna et al.*, 2012b]. Each of these terrestrial bodies represents a unique near-surface environment that can affect how thermal infrared emissivity measurements of those surfaces are acquired and interpreted for remote compositional analyses.

[1]Department of Geological Sciences, Brown University, Providence, Rhode Island, USA.
[2]Atmospheric, Oceanic and Planetary Physics, Clarendon Laboratory, University of Oxford, Oxford, UK.
[3]Geophysics and Planetary Geosciences Group, Jet Propulsion Laboratory, Pasadena, California, USA.

Corresponding author: K. L. Donaldson Hanna, Department of Geological Sciences, Brown University, Box 1846, Providence, RI 02912, USA. (ri_donaldson_hanna@brown.edu)

0148-0227/12/2012JE004184

[3] Thermal infrared spectra have diagnostic spectral features indicative of mineral composition that allow: (1) plagioclase to be identified and distinguished from other minerals and (2) different compositions of plagioclase to be identified from one another. Laboratory work by *Nash and Salisbury* [1991] demonstrated that the Christiansen feature (CF), an emissivity maximum diagnostic of composition [*Conel*, 1969], can be used to unambiguously identify plagioclase composition of fine powders and that the wavelength position of the CF is not affected by the vitrification of the surface. Other infrared studies [*Thompson and Wadsworth*, 1957; *Iiishi et al.*, 1971; *Ruff*, 1998] measured well-characterized samples of alkali and plagioclase feldspars and identified key differences in the reststrahlen bands, the fundamental molecular vibration bands due to stretching (Si-O-Si, Si-O-Al, Si-Si, and Si-Al) and bending (O-Si-O and O-Al-O), that can be used to distinguish between feldspar compositions. All of these studies focused on laboratory measurements made under ambient or Earth-like conditions, however laboratory measurements with different atmospheric and environmental conditions have shown that thermal infrared spectra are highly sensitive to the environments in which they are measured [e.g., *Logan et al.*, 1973; *Salisbury and Walter*, 1989; *Thomas et al.*, 2010; *Donaldson Hanna et al.*, 2012a].

[4] Here we present new thermal infrared emissivity measurements of five compositions of the plagioclase solid solution series measured under varying environmental conditions. The unique spectral features of each plagioclase composition are characterized as the temperature and pressure of the emission chamber are systematically varied to replicate ambient (Earth-like), half-vacuum (Mars-like), vacuum, and vacuum with cooled chamber (lunar-like) conditions. In addition, a relationship between the wavelength position of the CF and An# is developed under simulated lunar conditions for application to TIR data sets from the Moon.

2. Experimental Methods and Samples

[5] An emission chamber in the Planetary Spectroscopy Facility (PSF) at the University of Oxford Department of Atmospheric, Oceanic, and Planetary Physics has been built to simulate the temperatures and pressures experienced on the lunar surface [*Thomas et al.*, 2010]. The PSF chamber is attached to the potassium bromide (KBr) emission port window of a Bruker IFS-66v/S Fourier transform spectrometer. A KBr beamsplitter and a deuterated L-alanine doped triglyceride sulphate (DLaTGS) detector allow laboratory emissivity spectra to be collected at a resolution of 2 cm^{-1} over the 345–3030 cm^{-1} (3.3–29 μm) spectral range [*Thomas et al.*, 2010].

[6] Spectral measurements were made under four environmental conditions in the PSF chamber: ambient, half-vacuum, vacuum, and vacuum with cooled chamber. Ambient conditions simulate a terrestrial-like environment: samples are heated from below to ~350 K, the interior of the environment chamber is held at room temperature (~300 K), and the interior chamber pressure is ~1000 mbar of dry nitrogen gas (N2). A Mars-like environment is approximated under half-vacuum conditions: samples are heated from below to ~370 K, the interior of the environment chamber is held at room temperature, and the interior chamber pressure is ~5 mbar of N2. For vacuum measurements the sample is heated from below to ~420 K, the chamber interior is held to room temperature, and the interior chamber pressure is $<10^{-3}$ mbar. These measurements are intended to isolate the spectral effects due to vacuum pressures rather than simulating a particular body. To simulate the lunar environment (O1-SLE): samples are heated from below to ~500 K, the chamber interior is cooled with liquid nitrogen to ~120 K, and the interior chamber pressure is $<10^{-3}$ mbar.

[7] Samples were heated from below to temperatures optimized for obtaining high quality (high signal-to-noise ratio) spectra for each of the environmental conditions. In our heating from below experimental set-up, the decrease in chamber pressure creates a thermal gradient (a cold top layer over a hot bottom layer) as the interstitial gases between particulate materials are removed. This significantly changes the heat transfer mechanism from conduction to radiation, which more accurately reflects the physical environment of airless bodies.

[8] In order to understand the effects of the near-surface environment on fine particulate materials, our sample suite includes five well-characterized compositions of the plagioclase solid solution series (albite, oligoclase, andesine, labradorite, and anorthite) provided by Arizona State University (ASU) [*Christensen et al.*, 2000]. Since the fine fraction dominates the optical properties of lunar soils [*Pieters et al.*, 1993], samples were prepared as fine (<25 μm) particulate samples and measured in the PSF emission chamber under all four environmental conditions. Eight additional plagioclase samples of various compositions (Table 1) were prepared to the same particle size fraction (<25 μm) and measured in reflectance in Brown University's RELAB facility. These reflectance measurements are used to support the relationship between the An# of the ASU samples and the CF position measured under O1-SLE. The frequency (cm^{-1}) of the CF was identified for each plagioclase sample spectrum for each of the environmental conditions under which the sample was measured. A polynomial was fit to a portion of the ~1100–1400 cm^{-1} spectral range of each spectrum and the frequency of the maximum emissivity in the polynomial fit as seen in Figure 1 was used to represent the CF position. The spectral range and polynomial order were varied in order to best fit the emissivity value and shape of the CF of each sample spectrum. Due to the non-unique nature of identifying the CF position, the CF position can vary by ± 3 cm^{-1} as the spectral range and polynomial order are changed. In wavelength space, a $\pm$ 3 cm^{-1} error at ~7.5–8.0 μm equates to an error of ± 0.02 μm. This error in wavelength space is comparable to the maximum uncertainty of ± 0.03 μm in the CF position for particulate quartz measured in the PSF emission chamber [*Thomas et al.*, 2012].

[9] Mineral chemistry data for all of the plagioclase samples shown in Table 1 were obtained at the Massachusetts Institute of Technology (MIT) Electron Microprobe Facility using their JEOL JXA-8200 Superprobe. To obtain a representative mineral chemistry for each of the Arizona State University (ASU) samples, 10 to 15 grains greater than 125 μm in size were analyzed and averaged together. For the Brown and University of California Los Angeles (UCLA) samples, three locations (core, middle and rim) on grains 0.5–1.0 mm in size were analyzed and averaged together. Mineral chemistry and plagioclase composition (An#) for all of the samples are listed in Table 1. The variation in the mineral chemistry and plagioclase composition for each

Table 1. Mineral Sample Chemistry

Mineral Name	Source	SiO_2	Al_2O_3	FeO	MgO	CaO	Na_2O	K_2O	Total	An#[b]
Albite WAR0235[a]	ASU[c]	69.3	19.9	0.0	0.0	0.2	11.9	0.2	101.5	01
Oligoclase WAR5804[a]	ASU[c]	63.3	23.4	0.0	0.0	4.5	9.4	0.3	100.8	21
Andesine WAR0024[a]	ASU[c]	56.8	27.7	0.1	0.0	9.6	6.0	0.5	100.7	46
Labradorite BUR3080a[a]	ASU[c]	56.3	28.0	0.2	0.0	10.4	5.6	0.6	100.7	48
Anorthite BUR340[a]	ASU[c]	44.9	35.4	0.4	0.0	18.7	0.9	0.0	100.3	92
Albite	UCLA[d]	68.7	19.8	0.0	0.0	0.2	12.0	0.2	100.8	01
Oligoclase	UCLA[d]	63.7	22.9	0.0	0.0	4.0	9.4	0.6	100.6	18
Andesine	UCLA[d]	53.3	29.7	0.4	0.1	12.2	4.5	0.4	100.4	59
Labradorite	UCLA[d]	52.0	29.8	0.5	0.1	12.7	4.3	0.2	99.5	62
Labradorite	Brown	52.0	29.2	0.3	0.1	12.3	4.2	0.3	98.5	61
Labradorite	Brown	52.4	29.1	0.4	0.1	12.3	4.4	0.3	99.0	60
Bytownite	Brown	48.4	31.7	0.4	0.1	15.7	2.4	0.1	98.8	78
Bytownite	UCLA[d]	49.4	32.3	0.5	0.0	15.5	2.7	0.1	100.5	76

[a]Samples measured in emission chamber at the University of Oxford.
[b]Molar An# values multiplied by 100.
[c]*Christensen et al.* [2000].
[d]*Greenhagen* [2009].

sample is calculated by taking the standard deviation from the average mineral chemistry and An# and multiplying by two and are reported in Table 2.

3. Results

[10] Spectral emissivity measurements for each of the plagioclase solid solution series samples under the four environmental conditions defined above can be seen in Figures 2–4. The position of the CF identified for each plagioclase sample under each environmental condition is listed in Table 3.

3.1. Observed Spectral Changes

[11] The decrease in emission chamber interior pressure from ambient (1000 mbar) to half-vacuum (5 mbar) conditions is enough to create observable changes in the emissivity spectra. As seen in Figures 2–4, spectral contrast of the CF increases relative to the RB and the position of the CF shifts to higher wave numbers (shorter wavelengths). The spectral contrast and positions of the RB and transparency feature (TF), an emissivity minima caused by volume scattering in a spectral region of relative transparency between the principal RB [e.g., *Salisbury and Walter*, 1989], are unchanged.

[12] As the interior pressure of the emission chamber decreases from 5 mbar to $<10^{-3}$ mbar for vacuum measurements, four changes in the spectral character are observed: (1) the position of the CF shifts to significantly higher wave numbers, (2) the spectral contrast of the CF increases relative to the RB, (3) the spectral contrast of the RB in the ~1200–900 spectral range decreases while the spectral contrast of the RB in the ~800–400 spectral range either increase or remain the same and (4) the TF disappears. The frequencies of the RB absorptions appear to remain unchanged. For O1-SLE measurements, the interior pressure of the emission chamber remains at $<10^{-3}$ mbar as the interior temperature of the emission chamber is cooled. Two observations are made: (1) the CF shifts to even higher wave numbers and (2) the spectral contrast of the CF further increases while the spectral contrast of the RB in the ~1200–900 spectral range continues to decrease. A transparency feature at slightly higher wave numbers than the emissivity peak (marked by a green vertical line in Figure 4) is observed in the two Na-rich samples, oligoclase (An_{21}) and albite (An_{01}), measured under vacuum and O1-SLE conditions. Our results corroborate previous lab measurements made under ambient, vacuum, and other lunar-like conditions [e.g., *Logan et al.*, 1973; *Salisbury and Walter*, 1989; *Donaldson Hanna et al.*, 2012a] and highlight the sensitive nature of emissivity spectra to the environmental conditions under which they are measured.

3.2. Lunar Application: CF Position Versus An#

[13] Previous reflectance measurements of the plagioclase solid solution series measured under ambient conditions showed that the wavelength position of the Christiansen feature systematically shifts to shorter wavelengths with composition from Ca-rich to Na-rich compositions [*Nash and Salisbury*, 1991]. The wavelength position of the CF is strongly dependent on the degree of polymerization of silicate minerals with

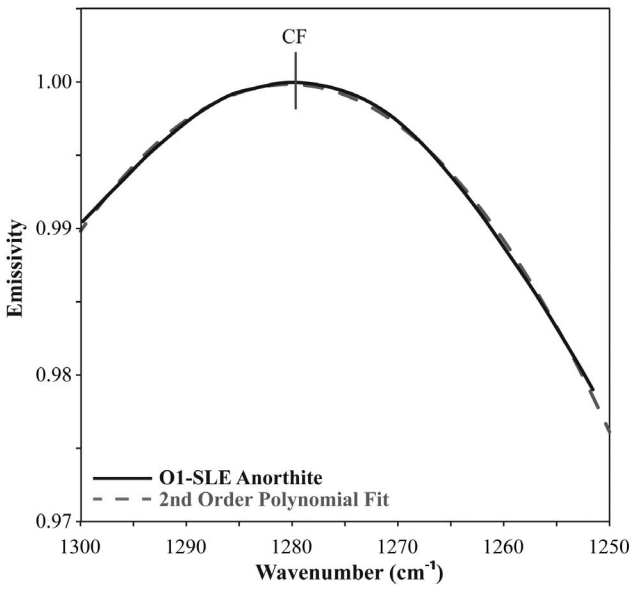

Figure 1. Anorthite spectrum measured under simulated lunar conditions (O1-SLE) plotted along with a 2nd order polynomial fit to the spectrum in order to determine the position of the Christiansen feature (CF). The CF position is identified as the frequency at the peak of the polynomial fit.

Table 2. Measured Variations in Mineral Chemistry (2× Standard Deviation)

Mineral Name	Source	SiO_2	Al_2O_3	FeO	MgO	CaO	Na_2O	K_2O	Total	An#[b]
Albite WAR0235[a]	ASU[c]	0.39	0.30	0.02	0.01	0.18	0.28	0.06	0.38	0.82
Oligoclase WAR5804[a]	ASU[c]	1.34	0.43	0.02	0.00	0.51	0.51	0.29	1.24	2.44
Andesine WAR0024[a]	ASU[c]	0.74	0.44	0.11	0.01	0.33	0.22	0.20	0.83	1.68
Labradorite BUR3080a[a]	ASU[c]	0.66	0.64	0.08	0.00	0.52	0.35	0.17	0.76	2.56
Anorthite BUR340[a]	ASU[c]	1.06	0.50	0.07	0.01	0.57	0.33	0.02	0.82	2.98
Albite	UCLA[d]	1.09	0.32	0.01	0.00	0.14	0.21	0.04	1.22	0.62
Oligoclase	UCLA[d]	0.28	0.37	0.02	0.00	0.02	0.15	0.02	0.22	0.18
Andesine	UCLA[d]	1.39	0.28	0.07	0.01	0.54	0.25	0.04	1.40	2.17
Labradorite	UCLA[d]	0.2	0.13	0.03	0.04	0.24	0.14	0.03	0.55	0.88
Labradorite	Brown	0.82	0.12	0.05	0.01	0.19	0.09	0.03	0.88	0.54
Labradorite	Brown	0.08	0.21	0.00	0.00	0.14	0.17	0.00	0.26	1.25
Bytownite	Brown	1.18	0.57	0.04	0.04	0.09	0.08	0.02	1.68	0.51
Bytownite	UCLA[d]	0.65	0.42	0.07	0.02	0.21	0.08	0.02	1.17	0.83

[a]Samples measured in emission chamber at the University of Oxford.
[b]Molar An# values multiplied by 100.
[c]*Christensen et al.* [2000].
[d]*Greenhagen* [2009].

framework silicates like quartz and feldspars having shorter wavelength CF positions than isolated silicate tetrahedra minerals like olivine [*Salisbury and Walter*, 1989]. Thus the observed systematic shift to shorter wavelengths observed in the plagioclase solid solution series is likely a result of minerals becoming more silica-rich from the substitution of Ca^{2+}, Al^{3+} with Na^{+}, Si^{4+} as compositions of plagioclase become more Na-rich.

[14] Laboratory emissivity measurements of the plagioclase solid solution series made under O1-SLE also show a systematic shift in the wavelength position of the CF as plagioclase compositions change from Ca-rich to Na-rich compositions (Figure 5). The identified wavelength positions of the CF for each of the plagioclase compositions can be related to the plagioclase composition (An#) of each sample. In Figure 6a, a linear relationship (O1-SLE CF position = 0.0033*An# + 7.4681) between An# and O1-SLE CF position is established with a R^2 value of 0.86832. While the linear trend is robust for the samples with An# ≥ 21, the albite (An_{01}) sample falls off the trend which could result from the transparency feature identified by the green vertical line in Figure 4. The TF affected the way the polynomial was fit to the emissivity spectra in determining the CF position and in doing so could have introduced a small error in the frequency at which the maximum emission was identified.

[15] To better understand the trend between the O1-SLE CF position and An#, the CF positions for an additional eight samples measured in RELAB are corrected to be comparable to the O1-SLE CF positions using the linear relationship (Ambient CF Position = 0.9502 * (O1-SLE CF Position) + 0.6778) previously established for a suite of silicate minerals measured under both ambient and O1-SLE conditions [*Donaldson Hanna et al.*, 2012a]. In Figure 6b, the addition of these estimated O1-SLE CF positions strengthen the linear relationship between the O1-SLE CF position and An#. However, these additional plagioclase samples will need to be measured under simulated lunar conditions to verify the observed linear trend. Error bar calculations for the CF position and An# were discussed previously in the Experimental Methods and Samples section.

Table 3. CF Positions (cm^{-1}) for Each of the Environmental Conditions

Mineral	An#	Ambient	Half Vacuum	Vacuum	O1-SLE
Albite	01	1300	1315	1328	1329
Oligoclase	21	1309	1322	1329	1330
Andesine	46	1261	1278	1306	1319
Labradorite	48	1262	1270	1306	1317
Anorthite	92	1219	1234	1272	1279

4. Discussion

[16] In order to approximate the lunar surface, our plagioclase samples include fine particulates (0–25 μm), not the

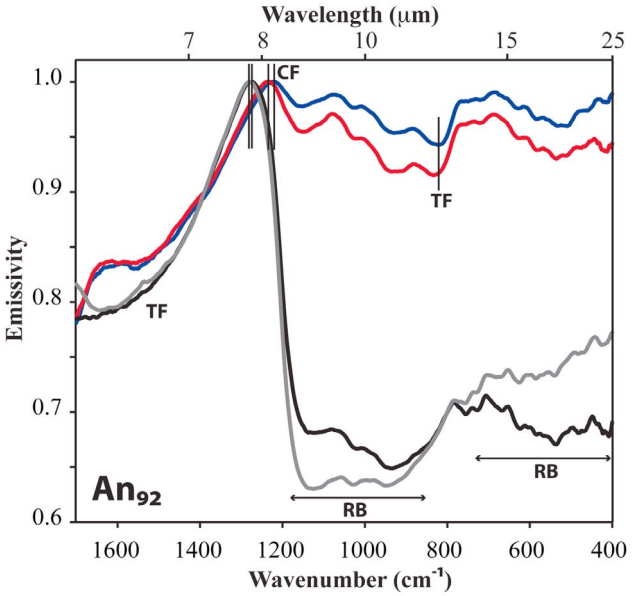

Figure 2. Emissivity spectra for anorthite (An_{92}). The blue is the spectrum measured under ambient conditions (Earth-like), red is the half-vacuum spectrum (Mars-like), black is the vacuum spectrum, and gray is the simulated lunar environment (O1-SLE) spectrum. Spectral features diagnostic of composition are as marked: Christiansen feature (CF), reststrahlen bands (RB), and transparency feature (TF) [e.g., *Lyon*, 1964; *Conel*, 1969; *Salisbury and Walter*, 1989].

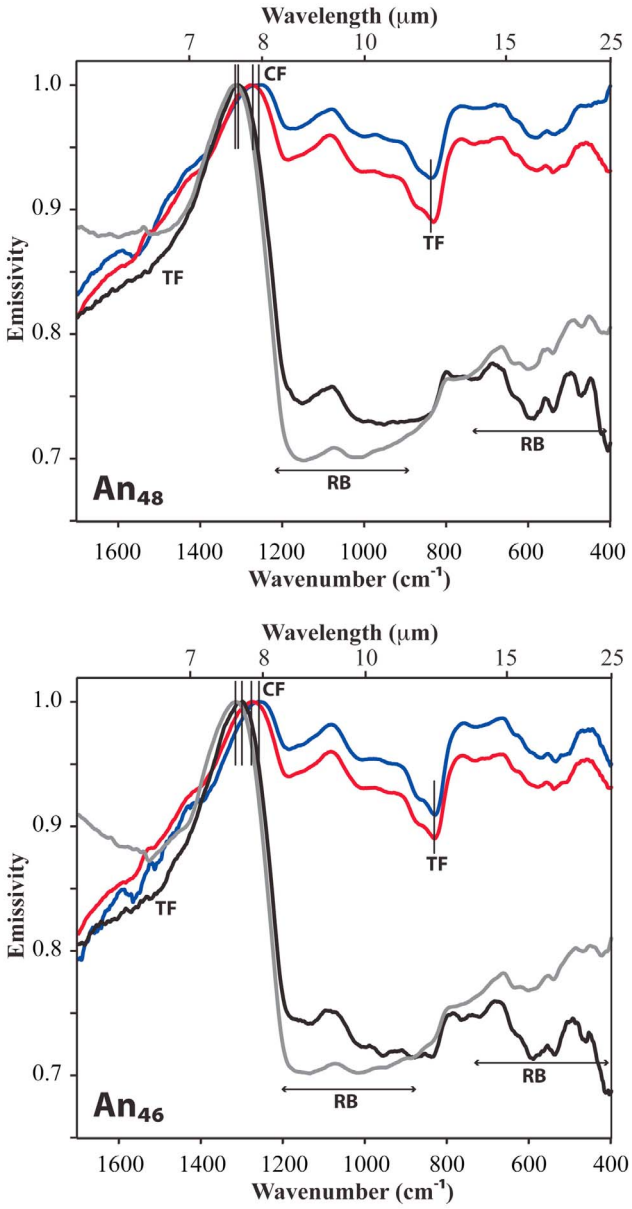

Figure 3. Emissivity spectra for labradorite (An_{48}) and andesine (An_{46}). For each plot, blue is the spectrum measured under ambient conditions (Earth-like), red is the half-vacuum spectrum (Mars-like), black is the vacuum spectrum, and gray is the simulated lunar environment (O1-SLE) spectrum. Spectral features diagnostic of composition are as marked: Christiansen feature (CF), reststrahlen bands (RB), and transparency feature (TF).

coarse particulate (>700 μm) samples measured under ambient conditions often used for modeling Martian TIR emissivity spectra. Our results, documenting the sensitivity of spectral features of particulate samples to environment, suggest that measurements of coarse particulate samples under varying environmental conditions should be further evaluated as well.

[17] For the thermal infrared spectral measurements in this study the sample heat source is located on the bottom of the sample cup. However, this single heat source arrangement does not fully replicate the near-surface thermal environment for airless terrestrial bodies. While radiating into space cools the uppermost surface, planetary surfaces are also heated by incident solar radiation. Thermal gradients are expected in a vacuum environment for porous particulate soils. New laboratory configurations at the University of Oxford PSF [*Thomas et al.*, 2012] and the Brown University RELAB [*Donaldson Hanna et al.*, 2012c] include solar-style heating from above to better replicate near-surface thermal environments. As these facilities become available, the plagioclase

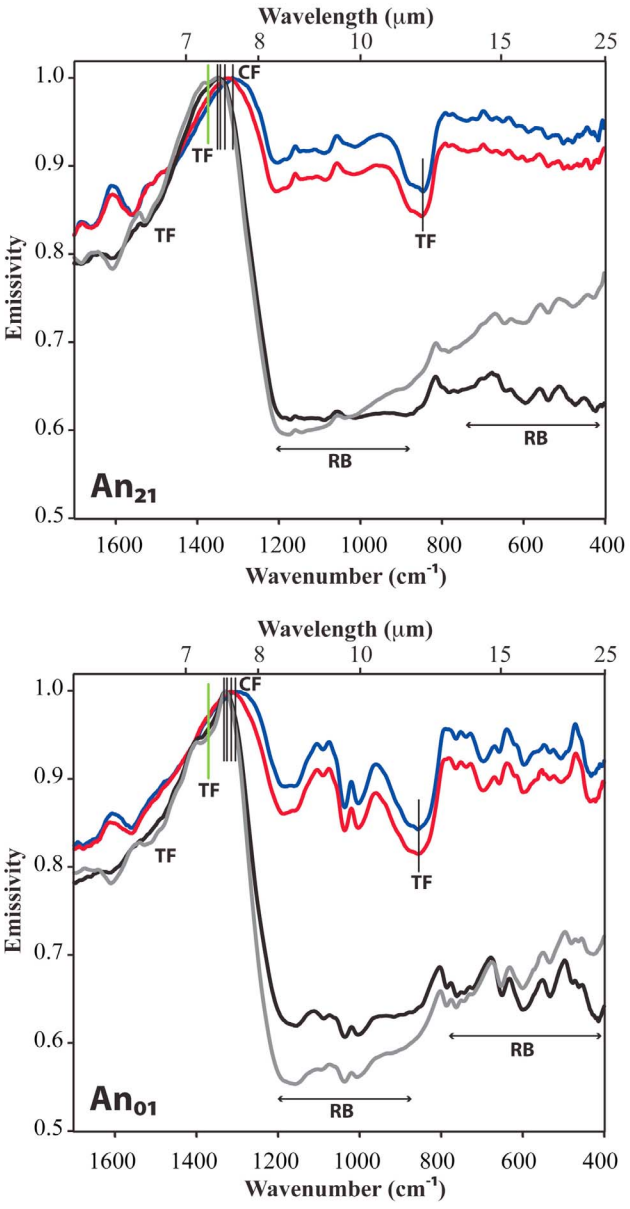

Figure 4. Emissivity spectra for oligoclase (An_{21}) and albite (An_{01}). For each plot, blue is the spectrum measured under ambient conditions (Earth-like), red is the half-vacuum spectrum (Mars-like), black is the vacuum spectrum, and gray is the simulated lunar environment (O1-SLE) spectrum. Spectral features diagnostic of composition are as marked: Christiansen feature (CF), reststrahlen bands (RB), and transparency feature (TF).

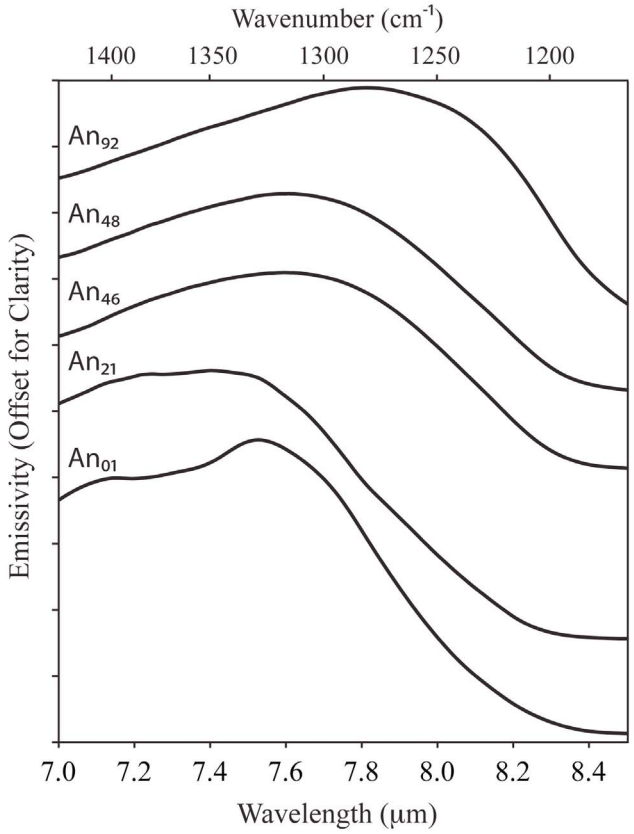

Figure 5. The Christiansen feature measured under O1-SLE conditions for the plagioclase solid solution series samples in this study. An# is listed for each sample as measured by electron microprobe analyses at MIT.

samples used in this study will be measured in the new laboratory arrangements to more fully understand the diagnostic spectral characteristics under more realistic environmental conditions.

[18] The linear trend between the wavelength positions of plagioclase samples measured under O1-SLE and the plagioclase sample composition established in Figure 6 allows the composition of plagioclase to be estimated from remote sensing data such as areas recently identified as pure plagioclase across the lunar surface [*Matsunaga et al.*, 2008; *Ohtake et al.*, 2009; *Pieters et al.*, 2009; *Donaldson Hanna et al.*, 2012b; *Yamamoto et al.*, 2012]. Initial analysis of these pure plagioclase regions using Diviner Lunar Radiometer thermal infrared data [*Greenhagen et al.*, 2010; *Donaldson Hanna et al.*, 2012b] show a range in CF values indicating compositional diversity. Our new spectral measurements of well-characterized plagioclase samples provide context for understanding this compositional diversity of plagioclase both locally and globally on the Moon, with implications for the nature of the lunar magma ocean and the subsequent chemical modification of the lunar crust.

5. Conclusions

[19] The character of TIR emissivity spectra change with changes in pressure and background temperature of the environment. As pressure decreases to $<10^{-3}$ mbar observed spectral changes include: (1) the CF position shifts to higher wave numbers (shorter wavelengths), (2) TF identified in the ~900–800 cm^{-1} (11–13 μm) spectral range disappear, (3) the spectral contrast of the CF increases relative to the RB, and (4) the spectral contrast of the RB in the ~1200–900 spectral range decreases while the spectral contrast of the RB in the ~800–400 spectral range either increase or remain the same. It is important to note that the small decrease in pressure between ambient (Earth-like) and half-vacuum (Mars-like) also introduces observable changes

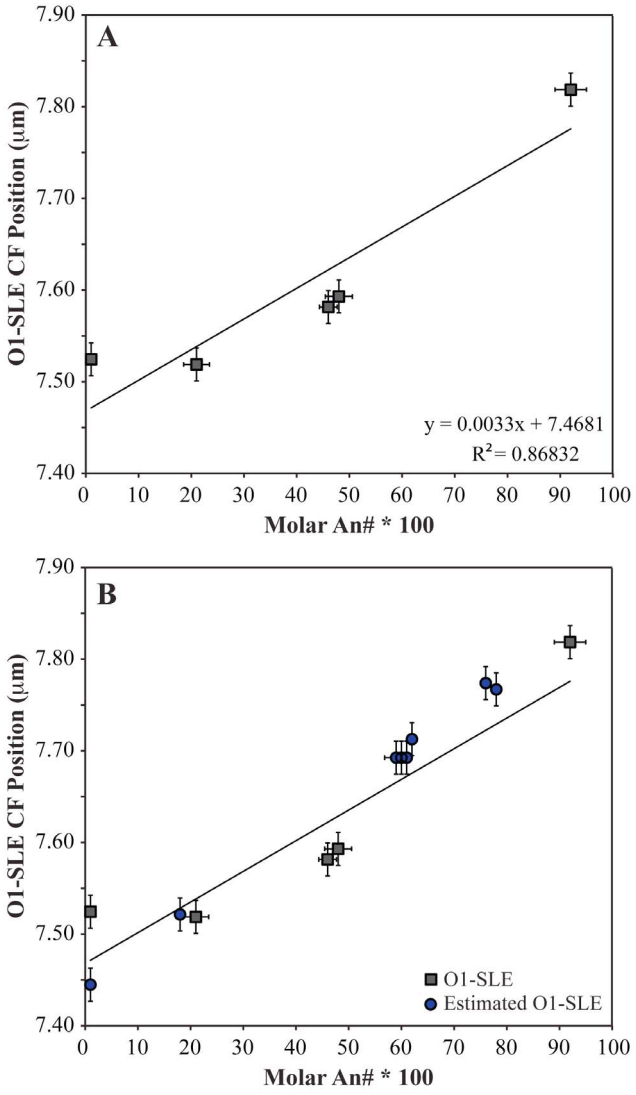

Figure 6. (a) The Christiansen feature position for a suite of plagioclase samples of varying composition measured under a simulated lunar environment (O1-SLE) plotted against the An# of each sample as measured by electron microprobe analyses. A linear trend with an R^2 value = 0.86832 is fit to the data. (b) The gray squares represent the five samples measured under O1-SLE and the blue circles indicate the estimated O1-SLE CF positions for the samples measured under ambient conditions in RELAB. For most of the blue circle data points, the horizontal error bars are smaller than the symbol size.

in emissivity spectra: (1) the CF position shifts to slightly higher wave numbers and (2) the spectral contrast of the CF increases. Since emissivity spectra of coarse particulate samples often used for modeling Martian surface compositions are measured under ambient laboratory conditions it will be important to measure coarse particulate samples under varying environmental conditions to further understand how the change in pressure between ambient and half-vacuum conditions may affect their spectral character.

[20] We established a linear trend between the wavelength position of the CF measured under a simulated lunar condition (O1-SLE) and the plagioclase composition (An#) that could be applied to current (Diviner) and future thermal infrared data sets of the Moon. As more plagioclase samples are measured under simulated lunar conditions the accuracy of this relationship between CF and An# will become more robust.

[21] **Acknowledgments.** We would like to extend our appreciation to Phil Christensen and Arizona State University for donating samples used in this study. A special thanks to Nilanjan Chatterjee at the MIT Electron Microprobe Facility for sample analyses. The authors would also like to thank Steve Ruff and the other anonymous reviewers for the thorough comments and suggestions that greatly improved this manuscript. K. L. Donaldson Hanna was supported by NASA grant ID NNX08AM75G. This research was supported in part by NLSI grant ID NNA09DB34A.

References

Bandfield, J. L., V. E. Hamilton, and P. R. Christensen (2000), A global view of Martian surface compositions from MGS-TES, *Science*, *287*, 1626–1630, doi:10.1126/science.287.5458.1626.

Christensen, P. R., J. L. Bandfield, V. E. Hamilton, D. A. Howard, M. D. Lane, J. L. Piatek, S. W. Ruff, and W. L. Stefanov (2000), A thermal emission spectral library of rock-forming minerals, *J. Geophys. Res.*, *105*, 9735–9739.

Conel, J. E. (1969), Infrared emissivities of silicates: Experimental results and a cloudy atmospheric model of spectral emission from condensed particulate mediums, *J. Geophys. Res.*, *74*, 1614–1634, doi:10.1029/JB074i006p01614.

Donaldson Hanna, K., and A. L. Sprague (2009), Vesta and the HED meteorites: Mid-infrared modeling of minerals and their abundances, *Meteorit. Planet. Sci.*, *44*, 1755–1770, doi:10.1111/j.1945-5100.2009.tb01205.x.

Donaldson Hanna, K. L., M. B. Wyatt, I. R. Thomas, N. E. Bowles, B. T. Greenhagen, A. Maturilli, J. Helbert, and D. A. Paige (2012a), Thermal infrared emissivity measurements under a simulated lunar environment: Application to the Diviner Lunar Radiometer Experiment, *J. Geophys. Res.*, *117*, E00H05, doi:10.1029/2011JE003862.

Donaldson Hanna, K. L., L. C. Cheek, C. M. Pieters, J. F. Mustard, M. B. Wyatt, and B. T. Greenhagen (2012b), Global identifications of crystalline plagioclase across the lunar surface using M^3 and Diviner data, *Proc. Lunar Planet. Sci. Conf.*, *43*, 1968.

Donaldson Hanna, K. L., C. M. Pieters, W. R. Patterson III, T. Hiroi, D. Moriarty, M. B. Wyatt, and C. Thompson (2012c), Asteroid and lunar environment chamber (ALEC): Simulated asteroid and lunar environments for measuring analog materials, *Proc. Lunar Planet. Sci. Conf.*, *43*, 2241.

Dowty, E., M. Prinz, and K. Keil (1974), Ferroan anorthosite: A widespread and distinctive lunar rock type, *Earth Planet. Sci. Lett.*, *24*, 15–25, doi:10.1016/0012-821X(74)90003-X.

Greenhagen, B. T. (2009), Thermal emission remote sensing of the Moon: Design and development of Diviner Lunar Radiometer compositional capabilities, PhD dissertation, 175 pp., Univ. of Calif., Los Angeles.

Greenhagen, B. T., et al. (2010), Global silicate mineralogy of the Moon from the Diviner Lunar Radiometer, *Science*, *329*, 1507–1509, doi:10.1126/science.1192196.

Hamilton, V. E., M. B. Wyatt, H. Y. McSween Jr., and P. R. Christensen (2001), Analysis of terrestrial and Martian volcanic compositions using thermal emission spectroscopy: 2. Application to Martian surface spectra from the Mars Global Surveyor Thermal Emission Spectrometer, *J. Geophys. Res.*, *106*, 14,733–14,746, doi:10.1029/2000JE001353.

Iiishi, K., T. Tomisaka, T. Kato, and Y. Umegaki (1971), Isomorphous substitution and infrared and far infrared spectra of the feldspar group, *Neues Jahrb. Miner. Abh.*, *115*, 98–119.

Logan, L. M., G. R. Hunt, J. W. Salisbury, and S. R. Balsamo (1973), Compositional implications of Christiansen frequency maximums for infrared remote sensing applications, *J. Geophys. Res.*, *78*, 4983–5003, doi:10.1029/JB078i023p04983.

Lyon, R. J. P. (1964), Evaluation of infrared spectrophotometry for compositional analysis of lunar and planetary soils, part II: Rough and powdered surfaces, *Rep. CR-100*, 264 pp., NASA, Washington, D. C.

Matsunaga, T., et al. (2008), Discoveries on the lithology of lunar crater central peaks by SELENE Spectral Profiler, *Geophys. Res. Lett.*, *35*, L23201, doi:10.1029/2008GL035868.

Mittlefehldt, D. W., T. J. McCoy, C. A. Goodrich, and A. Kracher (1998), Non-chondritic meteorites from asteroidal bodies, *Rev. Mineral. Geochem.*, *36*, 4.1–4.195.

Nash, D. B., and J. W. Salisbury (1991), Infrared reflectance spectra (2.2–15 μm) of plagioclase feldspars, *Geophys. Res. Lett.*, *18*, 1151–1154, doi:10.1029/91GL01008.

Ohtake, M., et al. (2009), The global distribution of pure anorthosite on the Moon, *Nature*, *461*, 236–240, doi:10.1038/nature08317.

Pieters, C. M., E. M. Fischer, O. Rode, and A. Basu (1993), Optical effects of space weathering: The role of the finest fraction, *J. Geophys. Res.*, *98*, 20,817–20,824, doi:10.1029/93JE02467.

Pieters, C. M., et al. (2009), Mineralogy of the lunar crust in spatial context: First results from the Moon Mineralogy Mapper (M3), *Proc. Lunar Planet. Sci. Conf.*, *40*, 2052.

Ruff, S. W. (1998), Quantitative thermal infrared emission spectroscopy applied to granitoid petrology, PhD dissertation, Ariz. State Univ., Tempe.

Salisbury, J. W., and L. S. Walter (1989), Thermal infrared (2.5–13.5 microns) spectroscopic remote sensing of igneous rock types on particulate planetary surfaces, *J. Geophys. Res.*, *94*, 9192–9202, doi:10.1029/JB094iB07p09192.

Thomas, I. R., N. E. Bowles, B. T. Greenhagen, T. D. Glotch, K. L. Donaldson Hanna, M. B. Wyatt, J. L. Bandfield, and D. A. Paige (2010), Emission measurements of lunar analogues for interpretation of returning data from the Diviner Lunar Radiometer on NASA's Lunar Reconnaissance Orbiter, *Proc. Lunar Planet. Sci. Conf.*, *41*, 1364.

Thomas, I., B. Greenhagen, N. Bowles, K. Donaldson Hanna, J. Temple, and S. Calcutt (2012), A new experimental setup for making thermal emission measurements in a simulated lunar environment, *Rev. Sci. Instrum.*, in press.

Thompson, C. S., and M. E. Wadsworth (1957), Determination of the composition of plagioclase feldspars by means of infrared spectroscopy, *Am. Mineral.*, *42*, 334–341.

Wood, J. A., J. S. Dickey, U. B. Marvin, and B. N. Powell (1970), Lunar anorthosites and a geophysical model of the moon, *Geochim. Cosmochim. Acta Suppl.*, *1*, 965–988.

Wyatt, M. B., and H. Y. McSween Jr. (2002), Spectral evidence for weathered basalt as an alternative to andesite in the northern lowlands of Mars, *Nature*, *417*, 263–266, doi:10.1038/417263a.

Yamamoto, S., et al. (2012), Global distribution trend of purest anorthosite on the Moon revealed by SELENE Spectral Profiler, *Proc. Lunar Planet. Sci. Conf.*, *43*, 1356.